An unsupervised method based on clustering and two-level dimensionality reduction for transfer function definition and design in Direct Volume Rendering

SIBGRAPI Paper ID: 99999

***Abstract*—Transfer function (TF) is one of the most researched topics in volume visualization. In the traditional Direct Volume Rendering (DVR) pipeline, a TF undertakes several roles, principally encompassing material classification and translating data into visual properties. A good TF is capable of generating precise classifications. It is widely known that this capability depends on the data domain. Multidimensional TFs have shown promise for improving classification power. However, the increase in the number of input attributes does not guarantee, by itself, better results. The identification of input data attributes that optimize classification accuracy typically demands user expertise. Moreover, designing a TF to highlight desired volume details is a complex task, particularly with multidimensional inputs. To address these challenges, we propose an unsupervised volume classification method that aids both TF definition and design, integrating feature selection, feature extraction, clustering, and pivot-based indexing. The method facilitates both the TF definition and design processes. The results of our work include an attribute similarity guide to TF definition, an easy-to-use volume exploration scheme based on an initial TF specification, a semi-automated data classification, and a modified 2D scatter plot view interface.**

I. Introduction

Direct Volume Rendering (DVR) is a powerful technology employed in computer science for visualizing three-dimensional scalar data grids, particularly in scientific and medical applications [1], [2]. The transfer function (TF) is a central component of the DVR pipeline and the object of study in this work. A TF translates volume data (such as density) to visual properties (such as color and opacity) displayed in rendered images [3].

When users interact with a DVR system, they often adjust TF parameters to reveal specific regions of interest within a dataset. A TF is a function in the "mathematical senses" whose input consists of a set of volume data attributes. The accuracy of classification is directly influenced by the data domain. Various studies [3]–[6] have already demonstrated that utilizing multidimensional TFs can significantly enhance discriminative power. Despite this, it is crucial to recognize that merely increasing the number of input attributes does not guarantee better classification results. There is no one-size-fits-all TF for each dataset. Consequently, this is usually left to the user's knowledge of the data domain [7].

Even after defining the TF, adjusting parameters remains essential to highlighting desired volume details. The design process is non-intuitive in one-dimensional space [5], [8], and this complexity further intensifies in higher-dimensional cases. Material classification benefits from higher-dimensional data, but it is difficult to specify TFs in such spaces [3], [5], [9], [10].

We propose a method that addresses the challenges of finding an appropriate TF for a given dataset and of assisting users in the design process. Our method adopts an unsupervised-based perspective that integrates feature selection, feature extraction, clustering, and pivot-based indexing. We also introduce an exploration scheme where users navigate over a set of volume details, which are semi-automatically classified and mapped to a modified 2D scatter plot view. Our major contributions can be summarized as follows:

- A feature selection strategy for the definition of multi-dimensional TF. Our method generates attribute rankings to furnish the user with information to select the most appropriate input data attributes.
- An effective and low-computational-cost TF design approach. We employ a semi-automated material classification to generate TF that requires minimal effort to adjust parameters.
- An easy-to-use volume exploration scheme. We provide an intuitive scatter plot view space for navigating over the classified data.

A. *Definition of Concepts*

In this paper, the term "feature selection" specifically refers to the group of dimensionality reduction (DR) techniques. Although some works in DVR use the term "feature" to denote regions or structures of interest within a dataset, we avoid this terminology here.

B. *Paper Organization*

The rest of this paper is organized as follows. Section II presents the related works. Section III describes the proposed method. The volume exploration scheme and the TF design interface are detailed in Section IV. Section V presents the results. The discussion of the results is provided in Section VI. Finally, the paper is concluded in Section VII.

II. Related works

Various aspects concerning TFs have been thoroughly discussed in the literature [3]. Our review focuses on methods that support user interaction in multidimensional design, especially those that apply machine learning, dimensionality reduction, and information visualization views.

A. Multidimensional data

A typical multidimensional TF consists of multivariate or derived input data. Multivariate attributes are obtained from the volume acquisition process, while derived attributes are usually calculated from material density data. The gradient stands out as the most commonly utilized derived attribute, with other examples including curvature [11], [12], size [13], [14], distance [15], texture [16] and statistical measures [17].

Selecting an optimal subset of attributes to maximize material classification accuracy is complex. [7] contend that there is no universally suitable TF for all cases. Considering all available attributes is impractical, as it may escalate computational costs and introduce noise, thereby diminishing classification results. This classical problem is known as "the curse of dimensionality". Dimensionality reduction is the most common attempt to address this challenge. Several approaches have resorted to such techniques to deal with multidimensional TFs [4], [18]–[21].

B. Transfer function design

1) 2D transfer function design: Histograms usually serve as the user interface for 2D TFs [9]. These interfaces generally represent the intensity-gradient magnitude and the low-high histograms. Various methods for automating histogram-based TF design have been proposed. [6] group spatially connected regions and associated gradient values with space coordinates to classify the datasets. Most approaches have combined histograms with clustering techniques, such as affinity propagation [22], hierarchical clustering [23], and the iterative self-organizing data analysis technique [24].

2) Multidimensional transfer function design: Approaches to designing multidimensional TFs normally conform to two primary strategies. The first entails furnishing an interface that enables the manipulation of all data attributes. One example of this interface type is the parallel coordinate plot (PCP). The second strategy involves leveraging dimensionality reduction techniques, such as those based on Multidimensional Scaling (MDS) and Principal Component Analysis (PCA).

[25] employed PCP in their exploration scheme, integrating viewer parameters and TF specifications into the design interface. [21] uses the same strategy with a local liner embedding technique for dimensionality reduction. Similarly, [26] proposed a hybrid interface design comprising PCP and a scatter plot generated via MDS.

[20] utilized a self-organizing map (SOM) and a radial-based function for TF design. SOM conducts dimensionality reduction through unsupervised learning, resulting in a map where neighborhood regions represent similar voxels. The user interaction involves drawing widgets in these regions. Likewise, [27] utilized a spherical SOM, enabling user interaction with the map lattice. [8] constructed a volume exploration space with subtree structures, using hierarchical clustering in a modified dendrogram. Afterward, [4] revisited these methods, augmenting the SOM result with a normalization cut step. The exploration space transforms into a cell map, with each region representing volume information associated with meaningful volume structures. Our approach shares similarities with the work of [4], but it utilizes an MDS-based technique and a density clustering algorithm to automate material classification, thereby generating a modified scatter plot view.

[28] proposed one of the earliest strategies employing supervised learning, implementing neural networks and support vector machines. [29] combined SOM and backpropagation neural networks for material classification. [30] used a Generative Adversarial Network (GAN) framework to compute models, addressing both TF specification and viewer position. Later, [31] combined GAN with Convolutional Neural Networks (CNN) to synthesize the exploration process. [32] developed an approach that utilizes CNN for generating visualizations from TF colorization. More recently, [10] introduced a design galleries approach employing deep learning and differentiable rendering to assist users in exploring the design space.

[33] developed a graph-based approach to identify significant volume structures, involving clustering features, constructing a material graph topology, and enhancing important structure rendering.

III. Method

In this section, we describe an unsupervised method for TF definition and design. Our method generates a semi-automated material classification and an initial TF specification. These elements are still combined to produce a simplified design interface and an intuitive volume exploration space.

Fig. 1 shows an overview of the proposed method. In a preprocessing step, the dataset is organized into a regular volume grid. Given that the input data is unlabeled, all techniques are applied from an unsupervised perspective. If multivariate data is not available, derived attribute extraction must be executed. The remainder of the method comprises the following steps: feature selection, feature extraction, clustering, and pivot-based indexing.

A. Feature selection

The first objective of our method is to facilitate the definition of the TF, or, in other words, to facilitate the selection of input data attributes.

Finding an appropriate multidimensional TF for a dataset is mainly a trial-and-error process. This task is typically supported solely by the user's knowledge.

Our method generates score rankings based on similarity measures between attributes. The user can thus make an assisted decision about the input attributes. Instead of manually examining all the combinations, the user can select the best

Fig. 1. Overview of the proposed unsupervised method for transfer function definition and design.

attributes presented in one of the rankings. We claim that feature-similarity information can make the process more efficient and intuitive. Here, it is assumed that given a set of data attributes $\mathbb{A}$ with $|\mathbb{A}| = d$, the feature selection process results in the choice of k attributes $\in \mathbb{A}$, where $k <= d$.

Algorithm 1 presents the technique used for the score rankings. The algorithm iteratively chooses the most dissimilar unselected attribute in comparison to those already selected. This task is performed until there are no remaining unselected attributes. The algorithm has the time complexity $\mathcal{O}(d^2 n)$, where d is the dimension (number of attributes) and n is the number of voxels.

```
Algorithm 1: Attribute score ranking.
  Input: set of attributes $\mathbb{A}$
  Output: list of selected attributes $R$
repeat
    $min \leftarrow \infty$
    $a_{selected} \leftarrow$ first $a \in \mathbb{A}$
    foreach $r \in R$ do
        $min_{ra} \leftarrow$ similarity-function($r$, $a$)
        if $min_{ra} < min$ then
            $min \leftarrow min_{ra}$
            $a_{selected} \leftarrow a$
        end
    end
    Append $a_{selected}$ to $R$
    Remove $a_{selected}$ from $\mathbb{A}$
until $\mathbb{A}$ is empty;
```

We employ the measures described by [34] as similarity functions in Algorithm 1, which are correlation coefficient, least squares regression error, and maximal information compression index (MICI).

The correlation coefficient measure is calculated as described in Equation 1.

$$\rho(x, y) = \frac{\text{cov}(x, y)}{\sqrt{\text{var}(x)\text{var}(y)}}, \qquad (1)$$

where ρ is the correlation coefficient score, var( ) denotes the variance of a random variable, and cov( ) is the covariance between two random variables x and y.

Equation 2 defines the least squares regression error measure.

$$e(x, y) = \text{var}(y)(1 - \rho(x, y))^2, \qquad (2)$$

where e is the least squares regression error score, var( ) denotes the variance of a random variable, and ρ is the correlation coefficient (Equation 1).

MICI measure is defined in Equation 3.

$$\begin{aligned} 2\lambda_2(x, y) &= (\text{var}(x) + \text{var}(y)) \\ &- \sqrt{(\text{var}(x)\text{var}(y))^2 - 4\text{var}(x)\text{var}(y)(1 - \rho(x, y)^2}, \qquad (3) \end{aligned}$$

where λ_2 is the maximal information compression index score, var( ) denotes the variance of a random variable, and ρ is the correlation coefficient (Equation 1).

Three rankings of attributes (correlation coefficient, least squares regression error, and MICI) are calculated for feature selection. Because of the lack of labeled data and the focus on user visual analysis, feature selection remains challenging in TF definition. We propose a heuristic outlined as follows:

- Set the number of k selected attributes based on the number of d available attributes, where $k \approx \sqrt{d}$.
- Analyze the classification quality using the ranking based on the MICI, followed by the rankings based on the correlation coefficient and the least squares regression error.
- If satisfactory results are not achieved, continue the search for TF, updating k iteratively to $k + 1$ and $k - 1$.

It is important to note that the strategy does not automate attribute selection. Instead, it empowers the user by providing resources for conducting the selection process. The user retains full responsibility for selecting the best attributes. Furthermore, our approach does not impose limitations on feature selection. Users have the freedom to make arbitrary choices based on their specific needs and preferences.

B. *Feature extraction*

Our method performs a second dimensionality reduction step that serves two primary purposes. Firstly, it structures a 2D interface for the TF design and the volume exploration space. Secondly, it prepares the data for the clustering step, which requires 2D input.

We employed a feature extraction technique in this step. Besides the dimensionality reduction, it minimizes information loss once the feature selection step removes irrelevant and redundant attributes.

FastMap [35], a classical MDS algorithm, is the feature extraction technique used. We take into account the three advantages of applying this technique: low time complexity cost even with large datasets [35], flexibility to handle high-dimensional datasets [35], and ability to preserve the clustering structure of the original data [36], [37]. Another advantage is that no input parameter is required. The time complexity of the FastMap algorithm is $\mathcal{O}(nk)$, where n is the total number of voxels and k, is the dimensionality of the target space.

Let d be the original dimensionality of input data, the algorithm projects n samples into a k-dimensional space, where $k <= d$. Here, n is the total number of voxels, d is the number of original attributes (dimensionality) and $k = 2$. FastMap is a recursive algorithm that can be succinctly described in the following steps:

1) Find the two points, named as pivots, furthest away from each other in a dataset.
2) Project the remaining points onto a hyperplane orthogonally positioned between the pivots.

Strategies capable of precisely identifying pivots have at least quadratic time complexity. To avoid compromising runtime, [35] developed a heuristic that is presented in Algorithm 2. It takes a set of points $\mathbb{O}$ and approximately finds the pair of points O_a and O_b that are the farthest from each other. In our approach, each point is a voxel, and thus, $\mathbb{O}$ is the set of all voxels. The algorithm considers only the values of selected attributes. A voxel's 3D position (x, y and z) is not used in any calculation.

Algorithm 2: Pivot searching of FastMap.

```
Input: $\mathbb{O}$
Output: Pivots $O_a$, $O_b$
$O_a \leftarrow$ random point $o \in \mathbb{O}$
$O_b \leftarrow$ point $o \in \mathbb{O}$ farthest from $O_a$
$O_a \leftarrow$ point $o \in \mathbb{O}$ farthest from $O_b$
```

C. Clustering

A major goal of our method is to simplify material classification and facilitate the highlighting of volume details. We address this objective by employing a classical density-based clustering algorithm, the DBSCAN [38].

DBSCAN is a widely utilized algorithm known for its success across various applications [39]. Nevertheless, its adoption in DVR comes with some caveats. The original version [38] exhibits a time complexity of $\mathcal{O}(n^2)$ in the worst case [39]. With practical usability in mind, we implemented a grid-based DBSCAN proposed by [40]. This version claims a time complexity of $\mathcal{O}(n \log(n))$.

Like the original algorithm [38], the 2D grid version also has $minPts$ and ε as input parameters. In this way, the user must fine-tune such parameters to best classify the volume data.

When this method step ends, each cluster comprises a subset of voxels that potentially represent a region of interest.

1) Grid-based DBSCAN of [40]: [40] introduces the concept of a grid to improve the efficiency of the clustering process, especially for high-dimensional datasets. The authors improve the scalability and efficiency of traditional DBSCAN by leveraging grid-based partitioning and density estimation techniques. Detailed explanations are provided in the works of [40] and [41]. The algorithm operates on a cell grid and comprises the tasks summarized next.

1) Grid partitioning. The first step involves partitioning the space into a grid of cells. Each cell represents a small portion of the entire space.
2) Density estimation. Within each cell, the algorithm calculates the density of points. The density is usually estimated using a distance threshold (ε) to determine the neighborhood of each point.
3) Identifying core points. Points with a density above a certain threshold ($minPts$) are considered core points. These core points are potential seeds for clusters.
4) Expanding clusters. Starting from a core point, the algorithm expands the cluster by iteratively adding neighboring points that also qualify as core points. The expansion continues until there are no more core points to be added.
5) Handling border points. Points that are within the ε neighborhood of a core point but do not meet the density requirement to be considered core themselves are classified as border points. Border points are assigned to the cluster of their nearest core point.
6) Handling noise. The points that are not core and do not belong to any cluster are considered noise points.

D. Pivot-based indexing

Our TF design interface revolves around a scatter plot view. Attempting to plot the entire dataset is impractical due to the high cognitive load and computational cost involved. To overcome this challenge, we implement a pivot-based indexing approach within each cluster identified by DBSCAN. Only the pivots within each cluster are plotted, thereby reducing visual density.

This step also serves as a second-level clustering process, refining each classified volume detail. Once the pivots are identified, each point in a cluster is assigned to the nearest pivot, as outlined in Algorithm 3. Therefore, a cluster is divided into sub-clusters represented by pivots.

Let $\mathbb{P}$ denote the set of all points within a cluster c, and $\mathbb{P}_s$ represent the selected pivots of the same cluster, every point $p \in \mathbb{P}$ is assigned to the sub-cluster of the nearest pivot $p_s \in \mathbb{P}_s$.

Algorithm 3: Finding sub-clusters within a cluster.

```
Input: Set of points $\mathbb{P}$ of a cluster $c$
Input: Set of pivots $\mathbb{P}_s$ of a cluster $c$
Output: Set of points $\mathbb{P}$ with associated sub-clusters
foreach $p \in \mathbb{P}$ do
    $p_s \leftarrow p$ nearest pivot in $\mathbb{P}_s$
    $p$ assigned to $p_s$'s sub-cluster
end
```

1) Sparse Spatial Selection: We use the Sparse Spatial Selection (SSS) for pivot-based indexing. This algorithm [42] is known for its straightforward implementation and low computational cost compared to other pivot-based techniques.

An overview of the SSS is shown in Algorithm 4. It identifies the points furthest from each other, termed pivots. Let $\mathbb{P}$ be a set of points, $alpha$ a distance factor within the interval $[0, 1]$, the first point $p_1 \in \mathbb{P}$ is added to the pivots $\mathbb{P}_s$. Subsequently, the algorithm traverses $\mathbb{P}$ to find additional pivots. With M representing the maximum distance between two arbitrary points, a point p is added to the pivots $\mathbb{P}_s$ only if $\forall p_s \in \mathbb{P}_s$, $\texttt{dist}(p, p_s) \geq M\alpha$, where dist is a distance function and p_s is a pivot $\in \mathbb{P}_s$.

To control the number of pivots, users can adjust the distance factor α. A smaller α value favours selecting a greater

Algorithm 4: Sparse Spatial Selection.

```
Input: Set of points $\mathbb{P}$
Output: Set of selected pivots $\mathbb{P}_s$
$\mathbb{P}_s \leftarrow p_1$
foreach $p \in \mathbb{P}$ do
    if $\forall p_s \in \mathbb{P}_s$, $dist(p, p_s) \geq M\alpha$ then
        $\mathbb{P}_s \leftarrow \mathbb{P}_s \cup \{p\}$
    end
end
```

number of pivots, while a value closer to 1 results in fewer pivots.

IV. Volume exploration space

Figure 2 illustrates the TF design interface. This system interface is a 2D scatter plot. Each circle represents a pivot selected by SSS. The positions provided in the FastMap results determine the points' position in the scatter plot. A pivot represents a central point within a cluster. It assigns size as a pivot's secondary property. The radius of a circle is calculated based on the number of voxels it represents, normalized using a logarithmic scale.

Our approach generates an initial specification for the TF using a predefined opacity value alongside a rainbow color scale. Each cluster is assigned a unique color.

Users can adjust the TF by following the What You See Is What You Get (WYSIWYG) principle. The lookup table is designed in such a way that the color and opacity of each pivot are directly mapped to the associated voxels, taking into account the clustering structure. Users can customize the color and opacity of any selected or not-selected elements.

Volume exploration happens through the selection of pivots. Our system dynamically adjusts the opacity of selected pivots to enhance visibility while concurrently reducing the opacity of non-selected elements. Users can interact with the system by making arbitrary selections. Even though hierarchical exploration is not the primary focus, our system supports it by enabling selections to be saved as groups, which can also be treated as selectable entities. This functionality empowers users to select pivots, clusters, and groups.

The iterative selection of nearby elements is essential for identifying details and regions of interest inside a volume. FastMap and DBSCAN naturally group instances that are more similar closer together, simplifying the identification process.

Our approach automates material classification. Therefore, we assume that each cluster, or in a more sophisticated analysis, each pivot, represents a relevant item. If the user is unsatisfied with the result, they can go back to selecting or deselecting any element or adjust the method parameters, which are:

- multidimensional TF definition,
- DBSCAN ε and $minPts$, and
- SSS distance factor α.

V. Results

A. Experimental Design

We conducted all the experiments on a computer equipped with an Intel Core I5 7200U, 8 GB RAM, running Ubuntu 22.04 64-bit, and an NVIDIA GeForce GT 940MX GPU.

For image rendering, we utilized a classical volume-ray casting algorithm with Blinn-Phong illumination and trilinear interpolation. The ray step is adjusted according to voxel spacing. Our runtime analysis reflects the average of five trials.

The system is implemented in C++, utilizing the Qt Framework and CUDA C/C++ for parallel processing. The implementation is available in online repositories.

Table I presents the datasets utilized in our experiments. These datasets are widely recognized within the volume visualization community and are publicly available through online repositories. The volume data consisted solely of material density, represented as intensity scalar values. The derived attributes are then used to generate multidimensional input. We consider 13 attributes, namely intensity, gradient magnitude, Laplacian magnitude, and 10 statistical measures computed from a local histogram. The statistical measures include absolute deviation, contrast, energy, entropy, inertia, Kurtosis, mean, skewness, standard deviation, and variance.

TABLE I

Volume datasets.

Dataset	Grid size	Total of voxels
Engine block	$256 \times 256 \times 256$	16,777,216
Knees	$379 \times 229 \times 305$	26,471,255
Tooth	$256 \times 256 \times 161$	10,551,296

The experiments generate rankings of attributes based on least squares regression error, MICI and correlation coefficient measures.

B. Runtime

Table II presents the runtimes for the proposed method applied to each dataset.

TABLE II

Runtime (in seconds) of the proposed method applied to each volume dataset.

	Block engine	Knees	Tooth
Rankings of attributes	*1540.50*	*2430.00*	*963.00*
Feature extraction	7.50	7.98	36.05
Clustering	51.52	102.77	19.42
Pivot-based indexing	2.23	3.15	1.33
Transfer function design interface	1.48	1.86	0.79

The feature selection process is not included in the runtime analysis, as it is performed manually. However, the calculation of attribute rankings is part of the analysis. It is pertinent to note that this step is computationally intensive compared

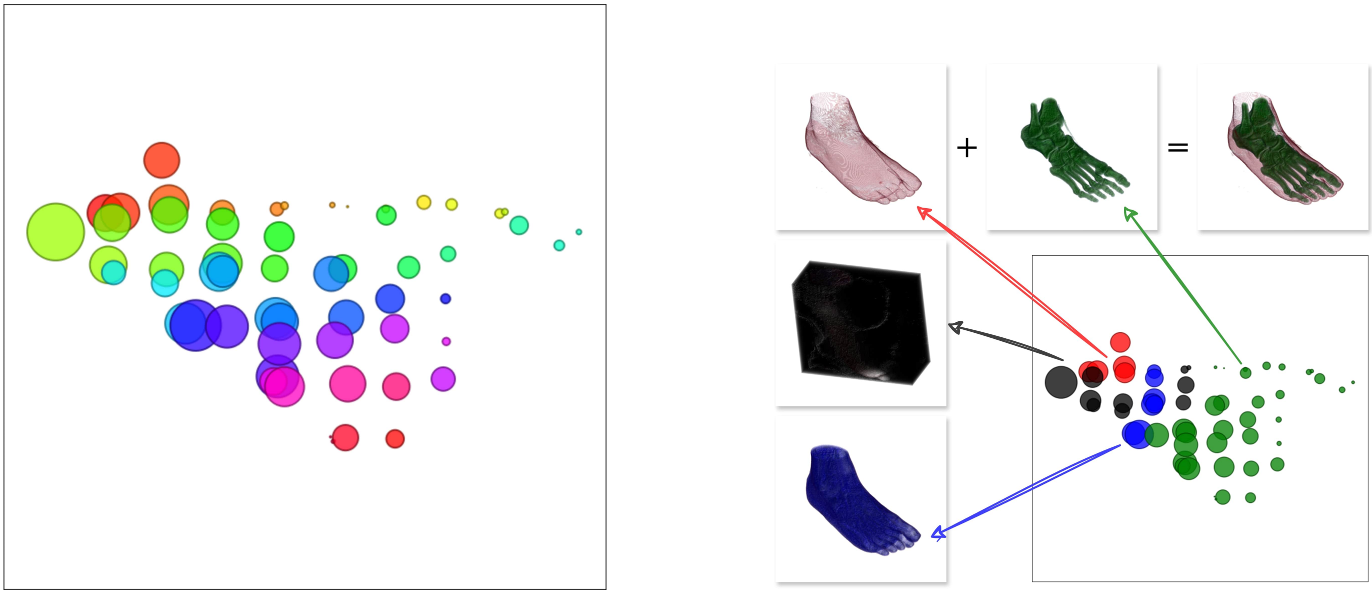
(a) Initial transfer function specification (semi-automatic generated).

(b) Fine-tune material classification after user adjustment.

Fig. 2. Transfer function design interface and volume exploration space of a right male foot dataset.

to other method steps, with attribute rankings taking 15–40 minutes to generate. The remaining steps of the method took under two minutes for all tested datasets.

C. Data classification

We use the heuristic proposed in Section III-A to search for a suitable TF for each dataset. Since the same number of attributes is available, we consistently began the investigation with $k = 4$, considering $d = 13$ (where $k \approx \sqrt{13}$) available attributes.

The DBSCAN parameter $minPts$ is default set [38] as 4 in all experiments. With the data normalized, we vary ε between $[0.2, 0.35]$ and SSS parameter α between $[0.8, 0.95]$ to simulate volume exploration.

1) Engine block dataset: Fig. 3 shows the volume exploration space generated for the engine block dataset. Each numbered group is a classified volume detail rendered as presented in Fig. 4. The method parameters are set as follows: $k = 4$, TF $=$ {intensity, skewness, gradient magnitude and variance}; $minPts = 4$; $\varepsilon = 0.35$; and $\alpha = 0.85$.

The rankings of attributes for the engine block dataset are shown in Table III. We obtained the best results with the one based on the correlation coefficient measure.

A volume exploration simulation is demonstrated in Fig. 5. It reveals different engine block components. The process happens from the initial setup presented in Fig. 3.

2) Knees dataset: A preliminary volume classification for knees datasets is presented in Fig. 6 and the related rendered details in Fig. 7. The method parameters are set as follows: TF $=$ {intensity, variance, absolute deviation, energy and contrast}; $minPts = 4$; $\varepsilon = 0.35$; and $\alpha = 0.9$.

Table V presents the rankings generated for the tooth dataset. We use the MICI measure ranking for the TF definition.

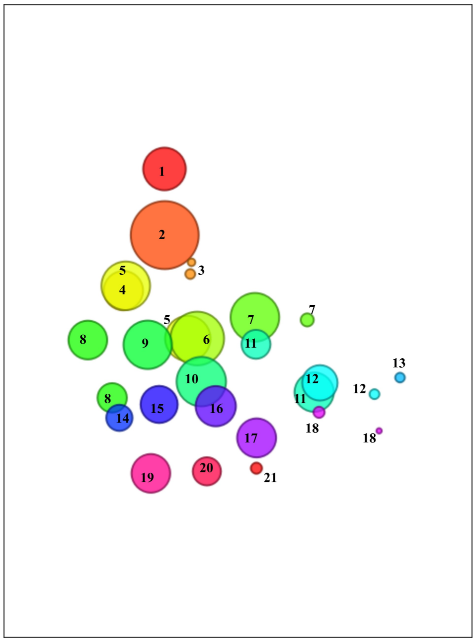

Fig. 3. Volume exploration space for the engine block dataset. Method parameters setup: transfer function $=$ {intensity, skewness, gradient magnitude and variance}; $minPts = 4$; $\varepsilon = 0.35$; and $\alpha = 0.85$.

By exploring the volume details, it is possible to group and identify bones and muscular structures. Fig. 8 illustrates these structures, which include parts of the femur, tibia, patella, fibula, thigh muscles, and knee muscles.

3) Tooth dataset: Fig. 10 presents visualizations of a tooth dataset classification. The method parameters are set as follows: TF $=$ {intensity, variance, absolute deviation, energy, contrast and entropy}; $minPts = 4$; $\varepsilon = 0.23$; and $\alpha = 0.9$.

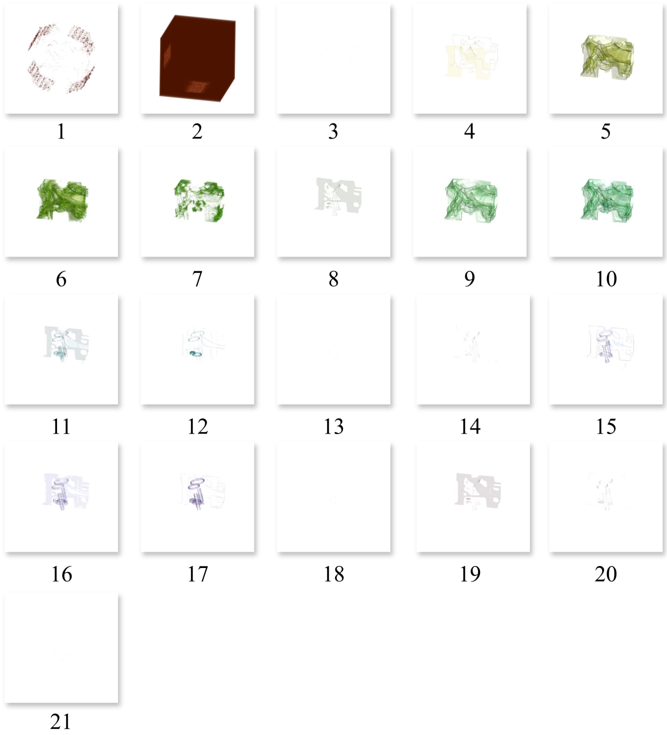

Fig. 4. Rendered volume classification details for the engine block dataset. Method parameters setup: transfer function = {intensity, skewness, gradient magnitude and variance}; $minPts = 4$; $\varepsilon = 0.35$; and $\alpha = 0.85$.

TABLE III
RANKINGS OF VOLUME DATA ATTRIBUTES FOR THE ENGINE BLOCK DATASET.

#	Least Squares Regression Error	Maximal Information Compression Index	Correlation Coefficient
1	Intensity	Intensity	Intensity
2	Energy	Variance	Skewness
3	Inertia	Absolute deviation	Gradient Magnitude
4	Entropy	Energy	Variance
5	Skewness	Contrast	Laplacian Magnitude
6	Mean	Entropy	Entropy
7	Absolute deviation	Gradient Magnitude	Energy
8	Laplacian Magnitude	Inertia	Inertia
9	Kurtosis	Kurtosis	Standard deviation
10	Standard deviation	Laplacian Magnitude	Mean
11	Gradient Magnitude	Mean	Kurtosis
12	Contrast	Skewness	Absolute deviation
13	Variance	Standard deviation	Contrast

Table V outlines the attribute dissimilarity rankings. The ranking based on the MICI measure is which one is chosen to support the TF definition.

Manually generated groups of related tooth details are presented in Fig. 11. It shows several discernible structures, including the enamel, pulp, dentin, crown, the entire tooth, and the fluid in which it is immersed.

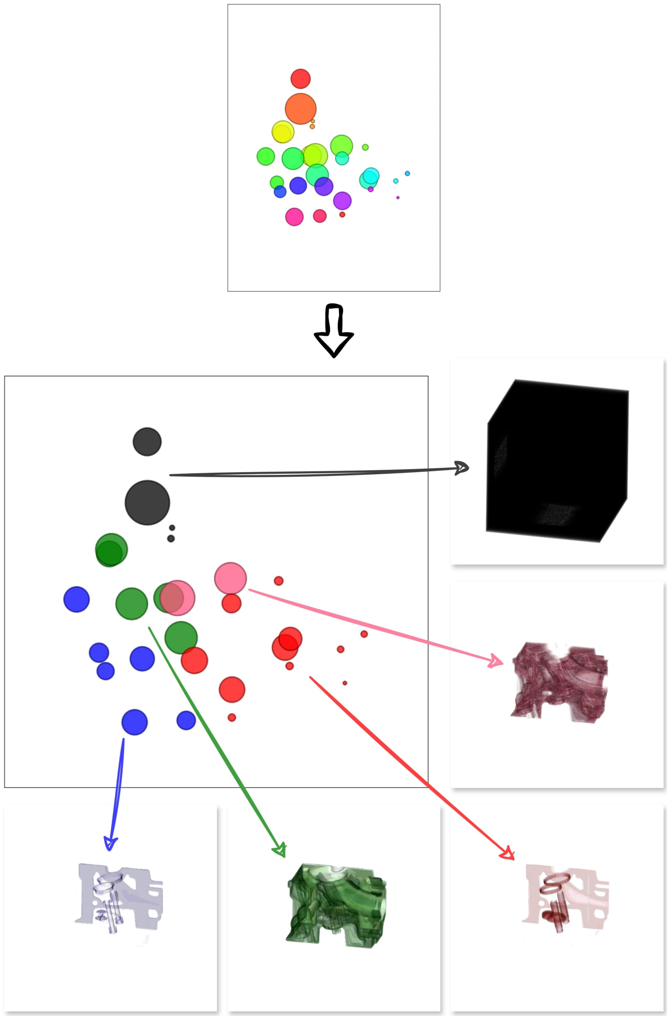

Fig. 5. Visual analysis of user-refined transfer function design and volume classification for engine block datasets. The volume details are manually grouped from an empirical perspective. Method parameters setup: transfer function = {intensity, skewness, gradient magnitude and variance}; $minPts = 4$; $\varepsilon = 0.35$; and $\alpha = 0.85$.

VI. Discussion

The two-level dimensionality reduction strategy effectively addresses challenges inherent in TFs. The first level offers guidance for TF definition, departing from the conventional approach reliant solely on user domain knowledge. This departure represents a significant advancement in the field. The second level simplifies the design interface.

While the feature selection heuristic shows promise in all experiments, the task ultimately remains the user's responsibility, which is a major limitation of our work. Investigating other unsupervised feature selection stop criteria may yield proper results, but there is a lack of investigation of these approaches in the TF context, warranting separate consideration in future analyses.

The parameters of DBSCAN significantly influence data classification. The parameter $minPts$ can assume a default value, $minPts = 4$ [38] since FastMap projects the data in

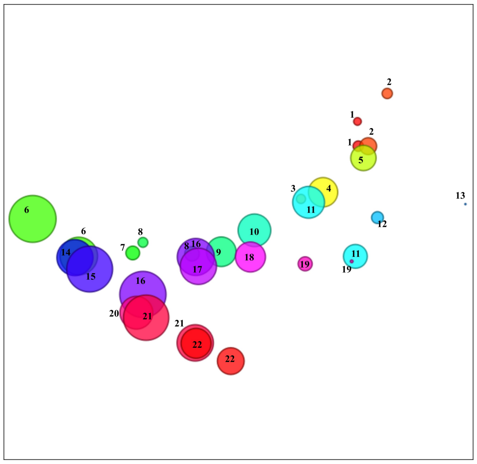

Fig. 6. Volume exploration space for the knees dataset. Method parameters setup: transfer function = {intensity, variance, absolute deviation, energy and contrast}; $minPts = 4$; $\varepsilon = 0.35$; and $\alpha = 0.9$.

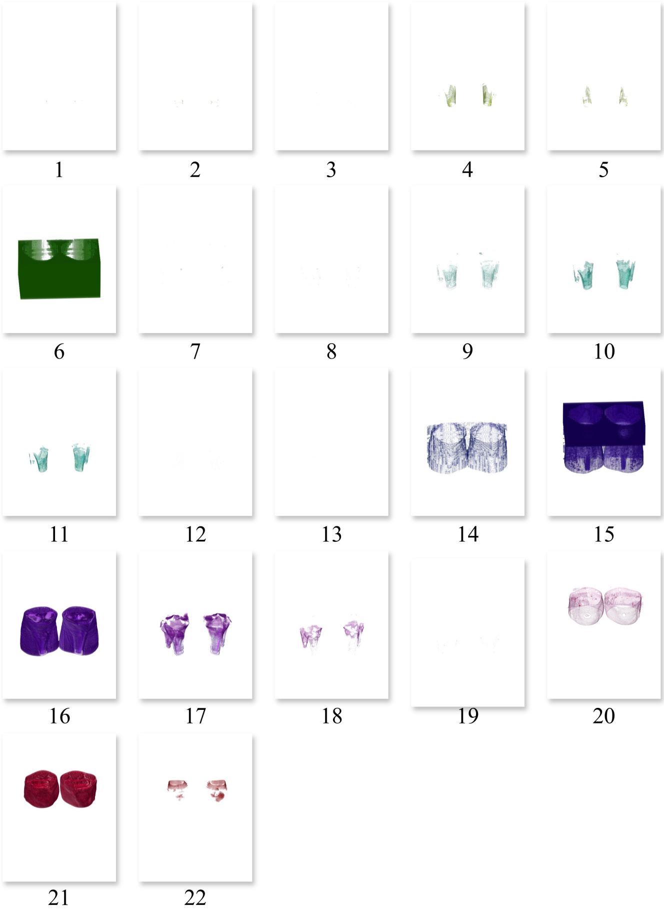

Fig. 7. Rendered volume classification details for the knees dataset. Method parameters setup: transfer function = {intensity, variance, absolute deviation, energy and contrast}; $minPts = 4$; $\varepsilon = 0.35$; and $\alpha = 0.9$.

a 2D space. The parameter ε requires a fine-tune adjustment, but its behavior is stable. Higher values of ε lead to fewer but larger clusters, while lower values increase the number of smaller clusters.

TABLE IV
RANKINGS OF VOLUME DATA ATTRIBUTES FOR THE KNEES DATASET.

#	**Least Squares Regression Error**	**Maximal Information Compression Index**	**Correlation Coefficient**
1	Intensity	Intensity	Intensity
2	Entropy	Variance	Variance
3	Energy	Absolute deviation	Skewness
4	Inertia	Energy	Entropy
5	Skewness	Contrast	Energy
6	Laplacian Magnitude	Entropy	Inertia
7	Mean	Gradient Magnitude	Standard deviation
8	Absolute deviation	Inertia	Laplacian Magnitude
9	Kurtosis	Kurtosis	Gradient Magnitude
10	Standard deviation	Laplacian Magnitude	Kurtosis
11	Gradient Magnitude	Mean	Absolute deviation
12	Contrast	Skewness	Mean
13	Variance	Standard deviation	Contrast

TABLE V
RANKINGS OF VOLUME DATA ATTRIBUTES FOR THE TOOTH DATASET.

#	**Least Square Regression Error**	**Maximal Information Compression Index**	**Correlation Coefficient**
1	Intensity	Intensity	Intensity
2	Energy	Variance	Variance
3	Inertia	Absolute deviation	Skewness
4	Entropy	Energy	Gradient Magnitude
5	Skewness	Contrast	Laplacian Magnitude
6	Laplacian Magnitude	Entropy	Energy
7	Mean	Gradient Magnitude	Inertia
8	Absolute deviation	Inertia	Standard deviation
9	Kurtosis	Kurtosis	Entropy
10	Gradient Magnitude	Laplacian Magnitude	Kurtosis
11	Standard deviation	Mean	Absolute deviation
12	Contrast	Skewness	Mean
13	Variance	Standard deviation	Contrast

Similarly, the adjustment of the SSS distance factor (α) follows the same behavior, with α being inversely proportional to the number of pivots within each cluster.

The practical implementation of the method is supported by minimal computational overhead, indicating favorable scalability for large datasets in size aspect. Despite the computational expense of the feature selection step in higher-dimensional cases, the remaining method steps can handle it.

VII. Conclusions

In this work, we presented a robust method for TF definition and design from an unsupervised data perspective. Our comprehensive approach covers the entire classification process, from feature selection to establishing a data domain, developing a TF design interface, and creating a simplified volume exploration space. We proposed a heuristic for

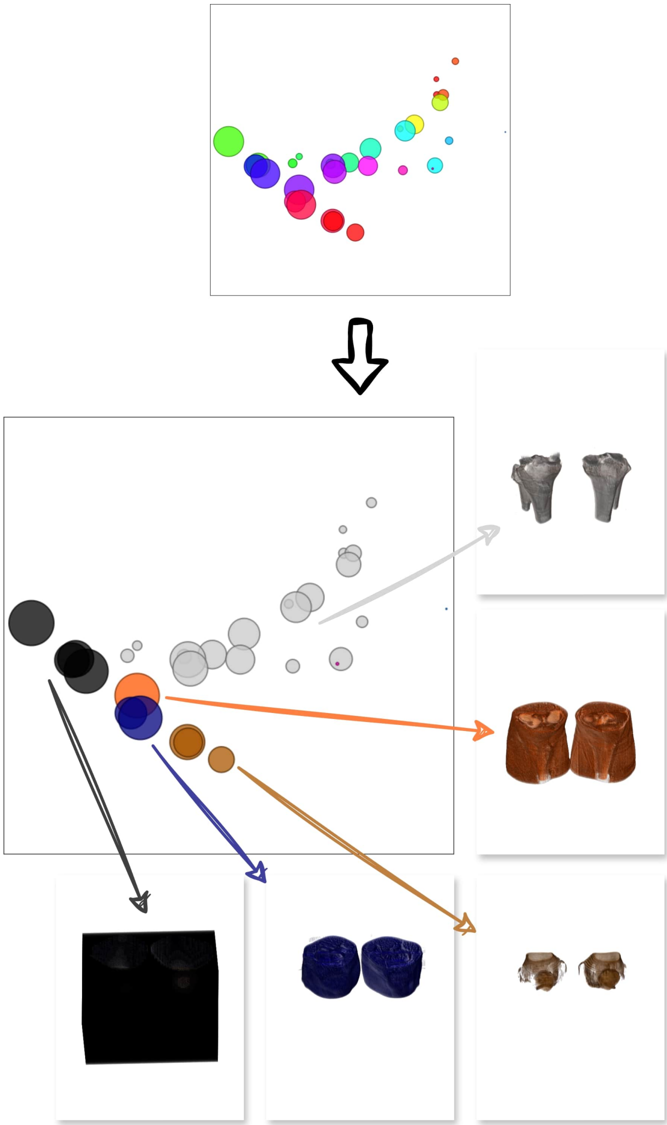

Fig. 8. Visual analysis of user-refined transfer function design and volume classification for knees dataset. The volume details are manually grouped from an empirical perspective. Method parameters setup: transfer function = {intensity, variance, absolute deviation, energy and contrast}; $minPts = 4$; $\varepsilon = 0.35$; and $\alpha = 0.9$.

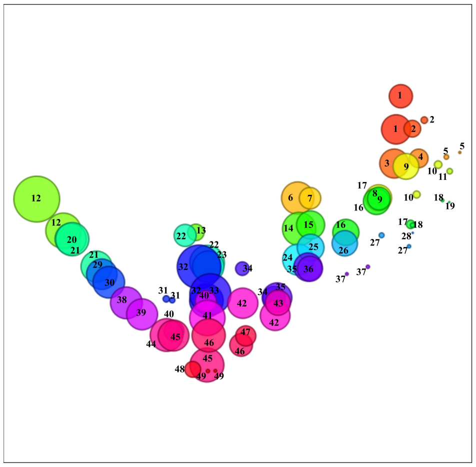

Fig. 9. Volume exploration space for the tooth dataset. Method parameters setup: transfer function = {intensity, variance, absolute deviation, energy, contrast and entropy}; $minPts = 4$; $\varepsilon = 0.23$; and $\alpha = 0.9$.

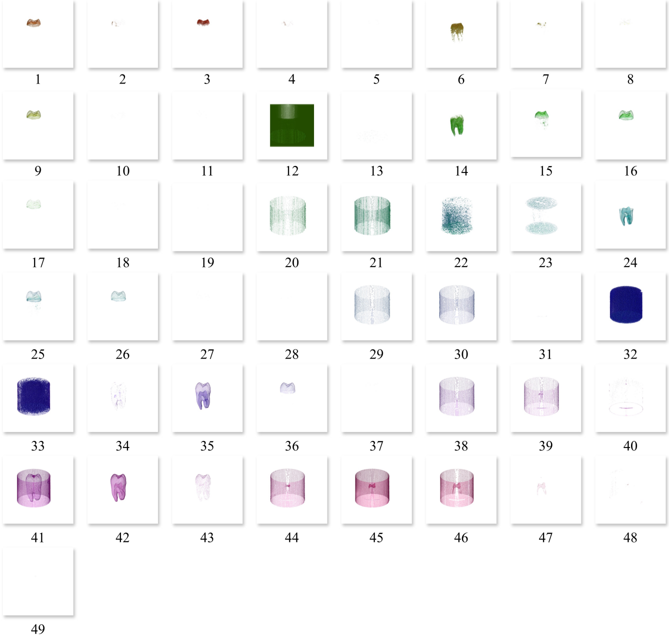

Fig. 10. Rendered volume classification details for the tooth dataset. The method parameters are set as follows: transfer function = {intensity, variance, absolute deviation, energy, contrast and entropy}; $minPts = 4$; $\varepsilon = 0.23$; and $\alpha = 0.9$.

feature selection based on similarity rankings of attributes, employed FastMap for efficient feature extraction, utilized DBSCAN for effective clustering, and leveraged SSS for pivot-based indexing. These techniques collectively facilitate semi-automatic classification and initial TF specification, forming the basis of our TF design interface and exploration system, as demonstrated through a scatter plot view.

The method exhibits minimal computational overhead, a brief runtime, and low storage requirements, highlighting its practicality and scalability for real-world applications. However, the current feature selection process, heavily reliant on user input, presents a limitation due to potential variability introduced by differing levels of user expertise. Nevertheless, the results are satisfactory in all experiments, given the unlabeled nature of the data. To address this, future work will focus on investigating advanced feature selection techniques and other stop criteria.

Another point of investigation is subjecting the method to handling large and high-dimensional datasets. The techniques included in the method are capable of operating well on datasets with these characteristics, and further practical investigation is needed in future studies to confirm its effectiveness.

Furthermore, we recognize the necessity to evaluate our proposed method using multivariate data, aiming to expand its applicability and robustness across diverse datasets.

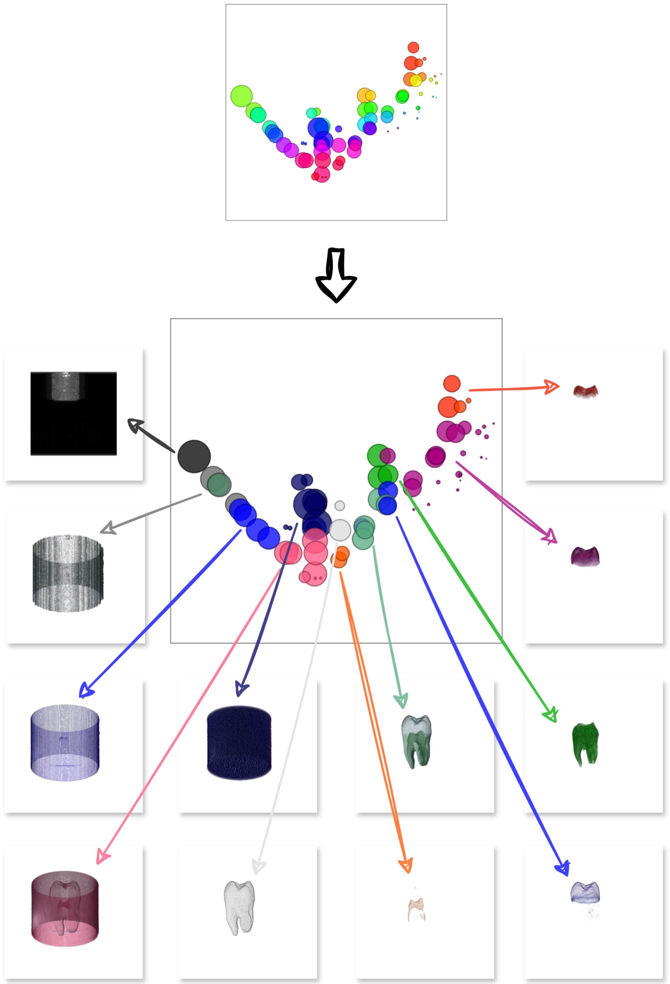

Fig. 11. Visual analysis of user-refined transfer function design and volume classification for tooth dataset. The volume details are manually grouped from an empirical perspective. The method parameters are set as follows: transfer function domain = {intensity, variance, absolute deviation, energy, contrast and entropy}; $minPts = 4$; $\varepsilon = 0.23$; and $\alpha = 0.9$.

Declaration of Generative AI and AI-assisted technologies in the writing process

During the preparation of this work the author(s) used ChatGPT 3.5 in order to improve readability and language of this paper. After using this tool/service, the author(s) reviewed and edited the content as needed and take(s) full responsibility for the content of the publication.

VIII. Introduction

SIBGRAPI 2025 [**?**].

A. Subsection Heading Here

Subsection text here.

1) Subsubsection Heading Here: Subsubsection text here.

IX. Conclusion

The conclusion goes here.

Fig. 12. SIBGRAPI - Conference on Graphics, Patterns and Images.

TABLE VI
An Example of a Table

One	Two
Three	Four

Acknowledgment

The authors would like to thank...

References

[1] T. T. Elvins, "A survey of algorithms for volume visualization," *ACM Siggraph Computer Graphics*, vol. 26, no. 3, pp. 194–201, 1992.

[2] C. Xu, G. Sun, and R. Liang, "A survey of volume visualization techniques for feature enhancement," *Visual Informatics*, vol. 5, no. 3, pp. 70–81, 2021. [Online]. Available: https://www.sciencedirect.com/science/article/pii/S2468502X21000358

[3] P. Ljung, J. Krüger, E. Groller, M. Hadwiger, C. D. Hansen, and A. Ynnerman, "State of the art in transfer functions for direct volume rendering," in *Computer graphics forum*, vol. 35, no. 3. Wiley Online Library, 2016, pp. 669–691.

[4] L. Cai, B. P. Nguyen, C.-K. Chui, and S.-H. Ong, "A two-level clustering approach for multidimensional transfer function specification in volume visualization," *Vis. Comput.*, vol. 33, no. 2, p. 163–177, feb 2017. [Online]. Available: https://doi.org/10.1007/s00371-015-1167-y

[5] H. Pfister, B. Lorensen, C. Bajaj, G. Kindlmann, W. Schroeder, L. S. Avila, K. Raghu, R. Machiraju, and J. Lee, "The transfer function bake-off," *IEEE Computer Graphics and Applications*, vol. 21, no. 3, pp. 16–22, 2001.

[6] S. Roettger, M. Bauer, and M. Stamminger, "Spatialized transfer functions," in *Proceedings of the Seventh Joint Eurographics / IEEE VGTC Conference on Visualization*, ser. EUROVIS'05. Goslar, DEU: Eurographics Association, 2005, p. 271–278.

[7] S. Arens and G. Domik, "A survey of transfer functions suitable for volume rendering." in *VG@ Eurographics*, 2010, pp. 77–83.

[8] L. Wang, X. Zhao, and A. E. Kaufman, "Modified dendrogram of attribute space for multidimensional transfer function design," *IEEE transactions on visualization and computer graphics*, vol. 18, no. 1, pp. 121–131, 2011.

[9] J. Kniss, G. Kindlmann, and C. Hansen, "Multidimensional transfer functions for interactive volume rendering," *IEEE Transactions on visualization and computer graphics*, vol. 8, no. 3, pp. 270–285, 2002.

[10] B. Pan, J. Lu, H. Li, W. Chen, Y. Wang, M. Zhu, C. Yu, and W. Chen, "Differentiable design galleries: A differentiable approach to explore the design space of transfer functions," *IEEE Transactions on Visualization and Computer Graphics*, vol. 30, no. 1, pp. 1369–1379, 2024.

[11] J. Hladuvka, A. König, and E. Gröller, "Curvature-based transfer functions for direct volume rendering," in *Spring Conference on Computer Graphics*, vol. 16, no. 5. Citeseer, 2000, pp. 58–65.

[12] G. Kindlmann, R. Whitaker, T. Tasdizen, and T. Moller, "Curvature-based transfer functions for direct volume rendering: Methods and applications," in *IEEE Visualization, 2003. VIS 2003.* IEEE, 2003, pp. 513–520.

[13] C. Correa and K.-L. Ma, "Size-based transfer functions: A new volume exploration technique," *IEEE transactions on visualization and computer graphics*, vol. 14, no. 6, pp. 1380–1387, 2008.

[14] S. Wesarg and M. Kirschner, "Structure size enhanced histogram," in *Bildverarbeitung für die Medizin 2009*. Springer, 2009, pp. 16–20.

[15] A. Tappenbeck, B. Preim, and V. Dicken, "Distance-based transfer function design: Specification methods and applications." in *SimVis*, 2006, pp. 259–274.

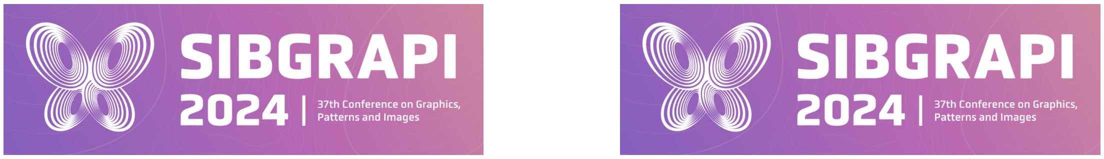
SIBGRAPI
2024
37th Conference on Graphics, Patterns and Images
SIBGRAPI
2024
37th Conference on Graphics, Patterns and Images

(a) Case I

(b) Case II

Fig. 13. SIBGRAPI - Conference on Graphics, Patterns and Images.

[16] J. J. Caban and P. Rheingans, “Texture-based transfer functions for direct volume rendering,” *IEEE Transactions on Visualization and Computer Graphics*, vol. 14, no. 6, pp. 1364–1371, 2008.

[17] M. Haidacher, D. Patel, S. Bruckner, A. Kanitsar, and M. E. Gröller, “Volume visualization based on statistical transfer-function spaces,” in *2010 IEEE Pacific Visualization Symposium (PacificVis)*. IEEE, 2010, pp. 17–24.

[18] A. Abbasloo, V. Wiens, M. Hermann, and T. Schultz, “Visualizing tensor normal distributions at multiple levels of detail,” *IEEE Transactions on Visualization and Computer Graphics*, vol. 22, no. 1, pp. 975–984, 2016.

[19] Y. Gao, C. Chang, X. Yu, P. Pang, N. Xiong, and C. Huang, “A vr-based volumetric medical image segmentation and visualization system with natural human interaction,” *Virtual Real.*, vol. 26, no. 2, p. 415–424, jun 2022. [Online]. Available: https://doi.org/10.1007/s10055-021-00577-4

[20] F. D. M. Pinto and C. M. D. S. Freitas, “Design of multi-dimensional transfer functions using dimensional reduction,” in *Proceedings of the 9th Joint Eurographics/IEEE VGTC conference on Visualization*, 2007, pp. 131–138.

[21] X. Zhao and A. Kaufman, “Multi-dimensional reduction and transfer function design using parallel coordinates,” in *Volume graphics. International Symposium on Volume Graphics*. NIH Public Access, 2010, p. 69.

[22] T. Zhang, Z. Yi, J. Zheng, D. C. Liu, W.-M. Pang, Q. Wang, J. Qin *et al.*, “A clustering-based automatic transfer function design for volume visualization,” *Mathematical Problems in Engineering*, vol. 2016, 2016.

[23] P. Sereda, A. Vilanova, and F. A. Gerritsen, “Automating transfer function design for volume rendering using hierarchical clustering of material boundaries.” in *EuroVis*, 2006, pp. 243–250.

[24] F.-Y. Tzeng and K.-L. Ma, “A cluster-space visual interface for arbitrary dimensional classification of volume data,” in *Proceedings of the Sixth Joint Eurographics - IEEE TCVG Conference on Visualization*, ser. VISSYM’04. Goslar, DEU: Eurographics Association, 2004, p. 17–24.

[25] M. Tory, S. Potts, and T. Moller, “A parallel coordinates style interface for exploratory volume visualization,” *IEEE Transactions on Visualization and Computer Graphics*, vol. 11, no. 1, pp. 71–80, 2005.

[26] H. Guo, H. Xiao, and X. Yuan, “Multi-dimensional transfer function design based on flexible dimension projection embedded in parallel coordinates,” in *2011 IEEE Pacific Visualization Symposium*. IEEE, 2011, pp. 19–26.

[27] N. M. Khan, M. Kyan, and L. Guan, “Intuitive volume exploration through spherical self-organizing map and color harmonization,” *Neurocomputing*, vol. 147, pp. 160–173, 2015.

[28] F.-Y. Tzeng, E. B. Lum, and K.-L. Ma, “An intelligent system approach to higher-dimensional classification of volume data,” *IEEE Transactions on visualization and computer graphics*, vol. 11, no. 3, pp. 273–284, 2005.

[29] L. Wang, X. Chen, S. Li, and X. Cai, “General adaptive transfer functions design for volume rendering by using neural networks,” in *International Conference on Neural Information Processing*. Springer, 2006, pp. 661–670.

[30] M. Berger, J. Li, and J. A. Levine, “A generative model for volume rendering,” *IEEE transactions on visualization and computer graphics*, vol. 25, no. 4, pp. 1636–1650, 2018.

[31] F. Hong, C. Liu, and X. Yuan, “Dnn-volvis: Interactive volume visualization supported by deep neural network,” in *2019 IEEE Pacific Visualization Symposium (PacificVis)*. IEEE, 2019, pp. 282–291.

[32] S. Kim, Y. Jang, and S.-E. Kim, “Image-based tf colorization with cnn for direct volume rendering,” *IEEE Access*, vol. 9, pp. 124 281–124 294, 2021.

[33] O. Sharma, T. Arora, and A. Khattar, “Graph-based transfer function for volume rendering,” in *Computer Graphics Forum*, vol. 39, no. 1. Wiley Online Library, 2020, pp. 76–88.

[34] P. Mitra, C. Murthy, and S. K. Pal, “Unsupervised feature selection using feature similarity,” *IEEE transactions on pattern analysis and machine intelligence*, vol. 24, no. 3, pp. 301–312, 2002.

[35] C. Faloutsos and K.-I. Lin, “Fastmap: A fast algorithm for indexing, data-mining and visualization of traditional and multimedia datasets,” in *Proceedings of the 1995 ACM SIGMOD international conference on Management of data*, 1995, pp. 163–174.

[36] I. K. Fodor, “A survey of dimension reduction techniques,” Lawrence Livermore National Lab., CA (US), Tech. Rep., 2002.

[37] I. Khan, J. Z. Huang, N. T. Tung, and G. Williams, “Ensemble clustering of high dimensional data with fastmap projection,” in *Pacific-Asia Conference on Knowledge Discovery and Data Mining*. Springer, 2014, pp. 483–493.

[38] M. Ester, H.-P. Kriegel, J. Sander, X. Xu *et al.*, “A density-based algorithm for discovering clusters in large spatial databases with noise,” in *kdd*, vol. 96, no. 34, 1996, pp. 226–231.

[39] E. Schubert, J. Sander, M. Ester, H. P. Kriegel, and X. Xu, “Dbscan revisited, revisited: why and how you should (still) use dbscan,” *ACM Transactions on Database Systems (TODS)*, vol. 42, no. 3, pp. 1–21, 2017.

[40] A. Gunawan and M. de Berg, “A faster algorithm for dbscan,” *Master’s thesis*, 2013.

[41] J. Gan and Y. Tao, “Dbscan revisited: Mis-claim, un-fixability, and approximation,” in *Proceedings of the 2015 ACM SIGMOD international conference on management of data*, 2015, pp. 519–530.

[42] O. Pedreira and N. R. Brisaboa, “Spatial selection of sparse pivots for similarity search in metric spaces,” in *International Conference on Current Trends in Theory and Practice of Computer Science*. Springer, 2007, pp. 434–445.